A New Robust Watermark Scheme using SIFT

Son Nguyen Thai
Faculty of Engineering and Technology
Tra Vinh University, Tra Vinh Province
Vietnam

ABSTRACT: *This paper proposed a new robust watermarking scheme using scale-invariant feature transform (SIFT) for the discrete wavelet transform (DWT) domain. In the proposed scheme, some SIFT feature regions are first determined in the original image. Then, these SIFT feature regions are transformed by using DWT transformation to generate the DWT coefficients, which is used to carry the watermark. In the receiver side, the watermark can be extracted correctly from the watermarked image. Experimental results show that the proposed scheme is withdraw under various attacks. In addition, in comparison with some exiting schemes, our proposed scheme obtains the stronger robustness than these schemes in regards with robustness and the visual quality.*

Keywords: DWT, High quality, SIFT, Watermarking

Received: 18 January 2016, Revised 22 February 2016, Accepted 2 March 2016

1. Introduction

Watermarking can hide secret information into the cover image to protect copyright of digital image, and the watermark is imperceptible. Then, to show the ownership of the image, the owner can extract the secret information from the embedded watermark. One of the important properties of watermarking is that it can be robustness against various types of attacks, i.e., geometric and signal processing attacks. Recently, many image watermark schemes [1-6] have been proposed. In [4], Bas et al. used the Harris detector to determine the image's the important points, and applied a Delaunay Tessellation to decompose the image into a set of disjoint triangles. For each triangle, one watermark is hidden. However, in their scheme, there is a difference between the important points extracted from the original image and from the attacked image. Thus, the embedded watermark cannot be extracted correctly in their scheme once the watermarked image is attacked. In [2], Li and Guo also used the Harris detector for determining the non-overlapped circular region for embedding the watermark. However, this scheme used the spatial domain for embedding watermark; thus, their scheme offers weak robustness under geometric attacks. To obtain stronger resilient against signal processing and geometric attacks, in [5], Seo and Yoo introduced a new watermarking schemes using multi-scale Harris detector. They decomposed the image into disjoint local circular regions, and selected some regions for carrying watermark. Lee et al. [3] applied SIFT to extract some local circular regions for watermarking. To embed the watermark, the pixels in these local circular regions are altered. However, these mentioned schemes [1-4] utilized the spatial domain for watermarking. Therefore, they offer the low watermark robustness under geometric and signal processing attacks. To overcome the weakness of these schemes [1-4], Li et al. [6] designed new watermarking scheme. Instead of using spatial domain for embedding watermark, in Li et al.'s scheme, DWT domain is applied. As a result, their scheme obtains high resilient against different watermark attacks.

To provide the high robustness watermarking scheme, in this paper, we design a new robust watermarking scheme. In the proposed scheme, SIFT algorithm is used to extract some SIFT regions for watermarking. To ensure higher robustness, DWT domain of these SIFT regions are utilized for embedding watermark. Experimental results demonstrate that the proposed scheme has the strong robustness to Salt & Pepper noise, Gaussian filtering, while maintain the high visual quality.

The rest of this paper is organized as follows: The SIFT technique [7] is review in Section 2. Section 3 describes the proposed scheme. Section 4 presents the experimental results and demonstrates the performance of the proposed scheme. Finally, Section 5 gives our conclusions.

2. SIFT Technique

In 2004, Lowe [7] first proposed SIFT technique which can maintain that the extracted feature points are stable to geometric transformations. The SIFT algorithm extracts the feature points from the scale space $L(x, y, \alpha)$, of image that is defined in Equation (1):

$$L(x, y, \alpha) = I(x, y) * G(x, y, \alpha), \tag{1}$$

where $I(x, y)$ is the digital image, * is the convolution operation, and $G(x, y, \alpha)$ is the variable-scale Gaussian kernel with standard deviation α. $G(x, y, \alpha)$ is defined in Equation (2):

$$G(x, y, \alpha) = \frac{1}{2\pi\alpha^2} e^{-(x^2+y^2)/2\pi^2} \tag{2}$$

The SIFT points are detected using scale-space extreme in the difference-of-Gaussian (DoG) function, $D(x, y, \alpha)$, which is computed Equation (3):

$$\begin{aligned} D(x, y, \alpha) &= I(x, y) * (G(x, y, k\alpha) - G(x, y, \alpha)) \\ &= L(x, y, k\alpha) - L(x, y, \alpha). \end{aligned} \tag{3}$$

where k is a constant multiplicative factor.

To determine the candidates, each point is compared its eight neighbors in the current image and the nine neighbors in the scale above and below, respectively. The point is selected only it is larger or smaller than all of these neighbors. In addition, the positions have low contrast or poorly localized, which are deleted by stability function. For more detail, readers should refer to [7].

3. Proposed scheme

Once the SIFT algorithm is used, several SIFT feature regions are determined in an image. To achieve more robustness of the embedded watermark, some small local regions should be removed. Only the region with the size larger than 60×60 pixels will be selected for embedding watermark as shown in Figure 1. If two areas are overlapped, only the one that, larger than 60×60 pixels, is reserved. This is because such regions are most appropriate for containing watermark sizes of 32×32 in the proposed scheme.

Figure 1. Example of selected SIFT feature regions

To achieve the high robustness of the watermark, three SIFT regions are used to embed the same copy of watermark. In addition, in the proposed scheme, the watermark embedding and the watermark detection algorithms are implemented in DWT domain. In the DWT transformation, the transformed image is obtained by repeatedly filtering the image on a row by row and column by column basis. After each level of DWT transformation, four sub-bands, i.e., *LL*, *LH*, *HL*, and *HH*, are obtained. Figure 2 shows an example of one-level DWT transformation.

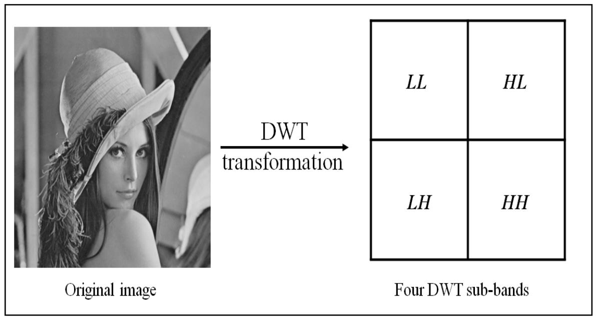

Figure 2. Example of one-level DWT transformation

In this paper, only one of two sub-bands, *LH* and *HL*, is used for carrying the watermark to obtain the trade-off between the robustness and visual quality. To better explain, in the rest of this paper, the sub-band HL is used for embedding watermark *W*. The proposed scheme can be divided into two phases, i.e., watermark embedding and watermark detecting, which are described in detail in Subsections 3.1 and 3.2.

3.1 Watermark Embedding

In this Subsection, the same copy of watermark is repeatedly embedded into three selected SIFT regions. The watermark embedding steps is shown in Figure 3.

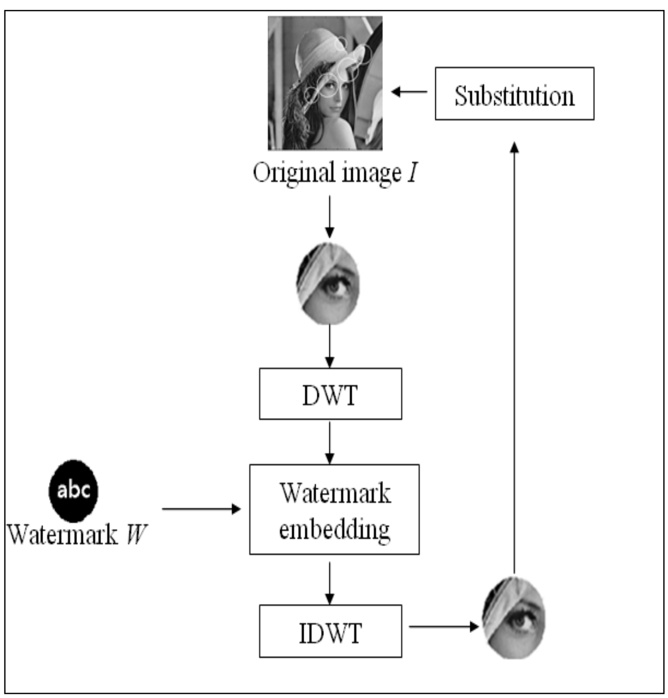

Figure 3. Watermark embedding processing

Step 1: Select three SIFT regions from the original image and the size of SIFT regions is larger than 60×60 pixel, and the size of the watermark W is 32×32.

Step 2: For each selected SIFT region, resize it to the size of 64×64, and apply one level DWT to generate four frequency sub-bands {*LL. LH, HL, and HH*}.

Step 3: Embed the watermark W by altering the coefficients in sub-band *HL*, as shown in Figure 4. Note that only the DWT coefficients inside the inscribed circle are altered for watermark.

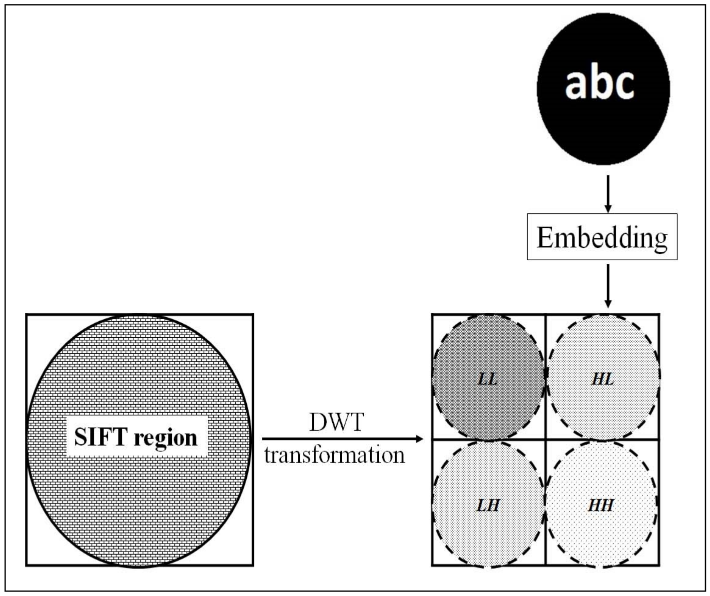

Figure 4. Demonstration of watermark embedding

Read watermark bit *W*(x, y), and the corresponding coefficient *HL*(x, y) with the same coordinate are selected in the sub-band *HL*. Then, the two first non-zero digits *Hi* of the fractional portion of *HL*(*x*, *y*) are determined to embed watermark bit *W* (*x*, *y*). For example, if *HL*(*x*, *y*) = 0.00**3**0**9**1, the value of *Hi* will be 39. Note that, since *Hi* is two first no-zero digits, thus, its value will be in range [11, 99]. The watermark bit *W(x, y)* is embedded into the value *Hi* using Equation (4).

$$Hi' = \begin{cases} \left\lfloor \dfrac{Hi+\Delta}{2} \right\rfloor & if\ W(x,y)=0\ and\ p<\Delta \\ \left\lfloor \dfrac{Hi-\Delta}{2} \right\rfloor & if\ W(x,y)=0\ and\ p>\Delta \\ \left\lfloor \dfrac{Hi+\dfrac{5\Delta}{2}}{2} \right\rfloor & if\ W(x,y)=1\ and\ p<\Delta \\ \left\lfloor \dfrac{Hi+\dfrac{3\Delta}{2}}{2} \right\rfloor & if\ W(x,y)=1\ and\ p>\Delta \end{cases} \quad (4)$$

Figure 5 shows the value of *Li'* based on the threshold Δ. Because the value of *Li* is from 11 to 99, the threshold Δ is set to 50 in this paper.

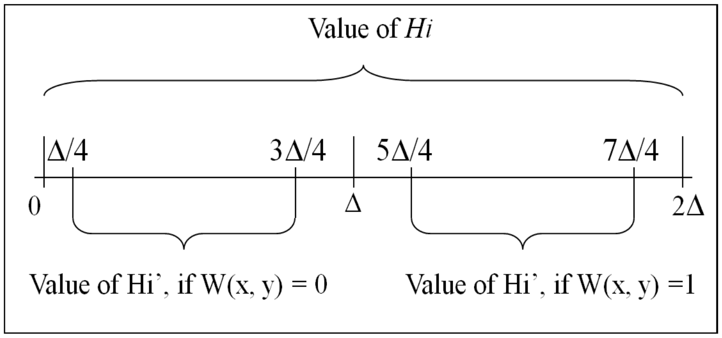

Figure 5. Value of *Hi'* based on threshold Δ
and the embedded watermark bit $w(x, y)$

Step 5: Apply one level IDWT to obtain the watermarked SIFT region. Resize this region back to its original size and substitute for the original SIFT region.

Step 6: Repeat steps 2 to 5 until three SIFT regions are processed completely.

3.2 Watermark Extracting

In this Subsection, watermark *W* is extracted from the watermarked image. First, three watermarked SIFT regions are extracted from the watermarked image as done in the embedding phase. Resize the selected region to the size of 64×64. Then, watermark is extracted from each watermarked SIFT regions as following:

Step 1: Apply one level DWT to generate four frequency sub-bands {*LL. LH, HL, and HH*}.

Step 2: For each coefficient $HL(x, y)$ in sub-band *HL*, the value *Hi'* is extracted as two first non-zero digits of the fractional portion of $HL(x, y)$. Note that only coefficients inside the inscribed circle of sub-band *HL* are processed. *W(*x*, y),* is extracted using Equations (5).

$$W(x,y) = \begin{cases} 0 & if \quad \Delta/4 \le Hi' \le 3\Delta/4 \\ 1 & if \quad 5\Delta/4 \le Hi' \le 7\Delta/4 \end{cases} . \tag{5}$$

Step 3: Make the final decision by the presentation of the extracted watermark.

4. Experimental Results

In this section, to demonstrate the performance of the proposed scheme, the experiments are implemented on standard image sized of 512×512. The watermark is a circular binary image size of 32×32, and three of SIFT regions are selected for watermark. Figure 7 shows performance of the proposed scheme in term of visual quality after the watermark is embedded into the original image.

Obviously, the proposed scheme obtained the invisibility, when the PSNR value is larger than 84 dB.

Figure 8 shows that the watermark can be extracted from all watermarked images under Salt and Pepper noise, JPEG 100, and Gaussian attacks with different parameters. As can be seen from Figure 8, the proposed scheme obtains the high value of normalized correlation coefficient (*NC*) that is larger than 0.9. Normalized correlation coefficient (*NC*) is used to measure the similarity between the embedded watermark *W* and the extracted watermark *W'*. It means that the proposed scheme can resilient to these attacks, whereas, ensuring the high visual quality larger than 84 dB as shown in Figure 7.

Table 3 shows the comparisons in term of watermark robustness between Li et al.'s scheme [6] and the proposed scheme. Table 3 shows that the proposed scheme obtains stronger robustness than that obtained by Li et al.'s scheme. Instead of embedding watermark in spatial domain, Li et al.'s scheme embedded the watermark into DWT domain.

(a) Original image

(b) Watermarked image (84.2 dB)

Figure 7. The image before and after watermarking

Attacks	**Li et al.'s scheme**	**Proposed scheme**
No attack	0.963	0.983
Median filter (33)	0.644	0.646
Shearing x-0%, y-5%	0.672	0.675
JPEG 100	0.942	0.982

Table 3. Comparisons of the robustness performance between Li et al.'s scheme and the proposed scheme

Figure 8. The extracted watermarks, and *NC* values under some watermark attacks

As a result, their scheme obtained higher robustness than that obtained by some previous schemes [2-5]. However, in Li et al.'s scheme, the difference value of between horizontal and vertical high frequency DWT coefficients is expanded to embed watermark bit. Therefore, if the value of one of the horizontal or the vertical high frequency DWT coefficients is modified, the extracted watermark bit will be changed. Conversely, in the proposed scheme, only the value of the horizontal or vertical high frequency DWT coefficient is altered to embed the watermark bit.

5. Conclusions

In this paper, a new image watermarking scheme is proposed to obtain high visual quality and strong robustness against various watermark attacks. In the proposed scheme, the SIFT feature regions are extracted, then a binary watermark image is repeatedly embedded into the DWT coefficients of the sub-band *HL* or *LH* of the selected SIFT feature regions. Experimental results demonstrate that the proposed scheme is resilient to various attacks, i.e. signal processing and geometric attacks. In addition, when compare the results of the proposed scheme with those obtained by some previous schemes; the proposed scheme achieves both higher visual quality and stronger robustness against various attacks.

References

[1] Deng, C. , Gao, X. B. , Li, X. L., Tao, D. C. (2009). A Local Tchebichef moments-based robust image watermarking, *Signal Process.*, 89, p. 1531-1539.

[2] Li, L. D., Guo, B. L. (2009). Localized image watermarking in spatial domain resistant to geometric attacks, *Int. J. Electron. Commun.*, 63, p. 123-131.

[3] Lee, H. Y. , Kim, H. , Lee, H. K. (2007). Robust image watermarking using local invariant features, *Optical Engineering*, 45, p. 1-10.

[4] Bas, P. , Chassery, J., Macq, B. (2002). Geometrically invariant watermarking using feature points, *IEEE Trans Image Process.*, 11, p. 1014-1028.

[5] Seo, J. ,Yoo, C. (2006). Image watermarking based on invariant region of scale-space representation, *IEEE Trans. Signal Process.*, 54, p. 1537-1549.

[6] Li, L. D. ,Qian, J. S. , Pan, J. S. (2011). Characteristic region based watermark embedding with RST invariance and capacity, *Int. J. Electon. Commun.*65, p. 435-442.

[7] G. Lowe, D. (2004). Distinctive image features from scale-invariant keypoints, *Int. Journal of Computer Vision*, 60 (2) 91-110.